Unveiling the Apparent "Negative Capacitance" Effects Resulting From Pulse Measurements of Ferroelectric-Dielectric Bilayer Capacitors

Zhan Liu, *Student Member, IEEE*, Hao Jiang, Brandon Ordway, and T. P. Ma, *Life Fellow, IEEE*

***Abstract*— Apparent 'Negative Capacitance' (NC) effects have been observed in some ferroelectric-dielectric (FE-DE) bilayers by pulse measurements, and the associated results have been published that claim to be direct evidence to support the quasi-static 'negative capacitance' (QSNC) idea. However, the 'NC' effects only occur when sufficiently high voltage is applied, and even exist in stand-alone FE capacitors. These results contradict the QSNC theory, as it predicts that once stabilized (requires a DE layer), the FE remains in the 'NC' state regardless of the applied voltage. In this letter, by the use of Nucleation-Limited-Switching (NLS) model, we present our results obtained from simulation of pulse measurements on samples that are similar to the published ones. The simulation results indicate that reverse polarization switching occurs upon the falling edge of the pulses, which leads to the apparent hysteresis-free NC effect. This work provides an alternative interpretation of the experimental results without invoking the QSNC theory.**

***Index Terms*— Ferroelectric, ferroelectric-dielectric bilayer, negative capacitance, Nucleation Limited Switching (NLS), numerical simulation.**

I. Introduction

SINCE first introduced in 2008 [1], the concept of ferroelectric 'Negative Capacitance' (NC) has become one of the hottest semiconductor research topics. Specifically, the Quasi-Static 'Negative Capacitance' (QSNC) theory [1] predicts the possibility of sub-60 mV/dec subthreshold swing (SS) in ferroelectric-gated field-effect transistors (FeFETs). Over the years, numerous experimental results have been reported to support the QSNC theory [2]–[10].

Among these experiments, a few involving pulse measurements of ferroelectric-dielectric (FE-DE) bilayer capacitors appeared to be most credible [8]–[10]. The researchers applied a sequence of pulses to the capacitors, and integrated the measured currents to obtain charge. The reason for using pulse measurement instead of quasi-static measurement is that charge-injection- assisted switching is suppressed with pulse measurement. Two possible switching patterns according to [8], [16], [17] are shown in Fig 1(a). The pulse measurement is faster than the time required for charge injection, such that the only possible switching pattern is Landau switching, and thus the NC effect arises. The typical charge-pulse relationship of the pulse measurement is depicted in Fig. 1(b). Three types of charges are defined: Q_{max}, the maximum charge; Q_D, released charge during the falling edge; and Q_{res}, the residual charge. Among them, Q_D is claimed to be the available free charge since both Q_{max} and Q_{res} include permanent polarization switching induced charge. Thus, the capacitance of the bilayer is claimed to be the slope of the $Q_D - V$ curve. A representative curve is qualitatively shown in Fig. 1(c). With high pulse amplitude, the slope of FE-DE stack is larger than that of the DE (capacitance boost effect), and no hysteresis is observed when sweeping back. These results provide strong support for the QSNC theory, based on the assumptions that (1) Landau switching is the only possible pattern, and (2) Q_D is not affected by permanent polarization switching.

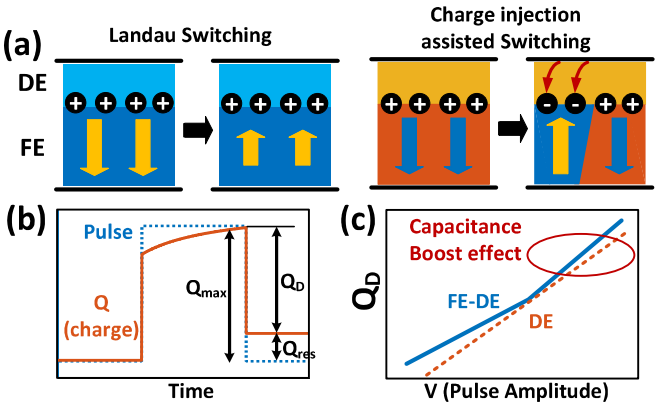

Fig. 1. (a) Two possible switching patterns claimed in [16]. Domain switching is claimed to be possible only with charge injection. (b) Schematic of the pulse measurement results. (c) The Q_D-V curves for FE-DE and DE with the same DE thickness.

In this work, we first show that domain switching could happen without charge injection. Then, by the use of the Nucleation Limited Switching (NLS) model [12], [13], we show that *reverse switching*, which happens at the falling edge of the pulse, can gives rise to the 'NC' effect observed in the imprinted FE capacitors [8] and FE-DE bilayer capacitors [8]–[10]. Our simulation results are consistent with

Manuscript received July 22, 2020; revised August 11, 2020; accepted August 28, 2020. Date of publication September 1, 2020; date of current version September 25, 2020. This work was supported in part by the U.S. National Science Foundation under Award 1941316. The review of this letter was arranged by Editor A. J. Naeemi. *(Corresponding authors: Zhan Liu; T. P. Ma.)*

The authors are with the Department of Electrical Engineering, Yale University, New Haven, CT 06511 USA (e-mail: zhan.liu@yale.edu; t.ma@yale.edu).

Color versions of one or more of the figures in this letter are available online at http://ieeexplore.ieee.org.

Digital Object Identifier 10.1109/LED.2020.3020857

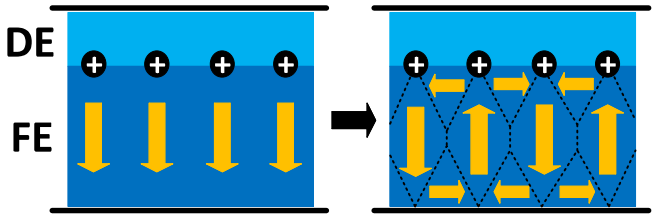

Fig. 2. Domain switching without FE-DE interface charge injection. The horizontal polarization acts as the compensation charge.

the reported experimental results presented in [8]–[10], and indicate that the pulse measurements only exhibit the 'NC' effects if reverse switching occurs.

II. Domain Switching Without Charge Injection

In the aforementioned switching patterns described in [16], the authors only considered polarization in the vertical direction, and the horizontal polarization is ignored. However, with the existence of horizontal polarization, it is possible to have domain structure, such as the one shown schematically in Fig. 2. The horizontal polarization has the effect of compensating the charge difference of vertical domains with inverse polarization. Both theoretical and experimental works have shown the existence of horizontal polarization [7], [18]–[20]. Furthermore, polycrystalline Hf-based ferroelectrics are unlikely to exhibit only uniform Landau switching. In general, it is reasonable to simulate pulse measurements with the domain switching model, instead of the Landau switching model.

III. Nucleation Limited Switching (NLS) Model

To simplify the simulation, all the interface charges and defects are ignored, and the bilayer capacitor is regarded as the FE and DE capacitors connected in series. The $Q - V_{app}$ relationship is thus expressed as:

$$V_{app} = V_{FE} + V_{DE} = \frac{(Q - P_{FE})}{C_{FE}} + \frac{Q}{C_{DE}} \tag{1}$$

in which Q is the free charge on the electrodes. $C_{FE} = \varepsilon_{FE}/d_{FE}$ and $C_{DE} = \varepsilon_{DE}/d_{DE}$ are the linear capacitance of FE and DE, respectively. P_{FE} is the ferroelectric polarization.

In NLS model, the ferroelectric layer is an ensemble of domains that switch independently [13]. For each domain, the switching is described as:

$$p(t, \tau) = 1 - \exp\left[-\left(\frac{t}{\tau}\right)^{\beta}\right] \tag{2}$$

where $p \in [0, 1]$ is the proportion of switched domains, β is a fitting parameter, and τ is the waiting time of nucleation that is a function of the field given by the empirical expression:

$$\tau = \tau_0 \exp\left[\left(\frac{E_a}{\eta E_{FE}}\right)^{\alpha}\right] \tag{3}$$

where, τ_0 is the minimum waiting time when the applied field is infinite, E_{FE} is the average field in the ferroelectric, E_a is the activation field, α is an empirical parameter, and η defines the relationship between the local field and the external field, while its distribution reflects the inhomogeneous nature of the polycrystalline ferroelectric. For $HfZrO_2$, the distribution of η is given by [13]:

$$f(\eta) = \frac{\frac{a}{b}\left(\frac{\eta}{b}\right)^{ac-1}}{B(c, d)\left(1 + \left(\frac{\eta}{b}\right)^{a}\right)^{c+d}}$$

where, a, b, c, and d are distribution parameters, and $B(c, d)$ is the beta function.

With these expressions, the polarization is computed as (where P_S is the saturated polarization):

$$P_{FE}(E_{FE}, t) = -P_S + 2P_S \int_0^{\infty} p(t, \tau) f(\eta) \, \mathrm{d}\eta \tag{4}$$

IV. Simulation

We use the finite difference method (FDM) to solve the equation. From (4), the finite difference of P_{FE} is:

$$\mathrm{d}P_{FE} = \frac{\partial P_{FE}}{\partial t}\mathrm{d}t + \frac{\partial P_{FE}}{\partial E_{FE}}\mathrm{d}E_{FE} \tag{5}$$

here, both $\mathrm{d}t$ and $\mathrm{d}E_{FE}$ are variables. However, in the time domain simulation, $\mathrm{d}t$ is the only independent variable, while $\mathrm{d}E_{FE}$ is a function of $\mathrm{d}t$. Thus, we need to calculate both $\mathrm{d}E_{FE}$ and $\mathrm{d}P_{FE}$ as functions of $\mathrm{d}t$. To do this, we notice that $\mathrm{d}E_{FE}$ is also a function of $\mathrm{d}P_{FE}$, given that $\mathrm{d}E_{FE} = (dQ - dP_{FE})/\varepsilon_{FE}$. From (1), we have $\mathrm{d}Q = (\mathrm{d}P_{FE}C_{DE})/(C_{FE} + C_{DE})$ when V_{app} is fixed (pulse measurement). With these two equations and (5), we are able to calculate $\mathrm{d}E_{FE}$ as:

$$\mathrm{d}E_{FE} = -\frac{\frac{\partial P_{FE}}{\partial t}\mathrm{d}t}{\left(1 + \frac{\varepsilon_{DE}d_{FE}}{\varepsilon_{FE}d_{DE}}\right)\varepsilon_{FE} + \frac{\partial P_{FE}}{\partial E_{FE}}}$$

The derivatives of P_{FE} with respect to t and E_{FE} are calculated from (2), (3), and (4). In some extreme cases, $\mathrm{d}E_{FE}$ is too large so that $\partial P_{FE}/\partial E_{FE}$may change significantly between E_{FE} and $E_{FE} + \mathrm{d}E_{FE}$. In such cases, we adjust the step of $\mathrm{d}E_{FE}$ and update $\partial P_{FE}/\partial E_{FE}$ until the condition is fulfilled.

The polarization state of each domain is recorded throughout the simulation. Before a pulse is applied, we calculate the effective 'time' $t_{0,i}$ of each domain based on (2) and the current value of E_{FE}. These $t_{0,i}$ are used as the starting points for the calculation, assuming the corresponding polarization states are the result of applying the current E_{FE} for $t_{0,i}$ time. This procedure solves the problem when partially switched polarization is the initial condition.

In this simulation, we use HZO as the FE, and Al_2O_3 as the DE. The corresponding parameters are: $\alpha = 3.73$, $\beta = 2.06$, $\tau_0 = 236\ ns$, $E_a = 1.94\ MV/cm$, $P_S = 27\mu C/cm^2$, $\varepsilon_{FE} = 30\varepsilon_0$, $\varepsilon_{DE} = 8\varepsilon_0$, $d_{FE} = 10\ nm$, $a = 9.0986$, $b = 1.3935$, $c = 1.1101$, and $d = 15.197$, where ε_0 is the vacuum permittivity [13].

V. Results and Discussion

A. Stand-Alone Imprinted FE Capacitor

Fig. 3 shows the simulation results of an imprinted FE capacitor, which represents the BTO sample depicted as the inset of Fig. 2(f) in [8]. To simplify the simulation, the imprint is simulated as the shifts of the coercive voltage.

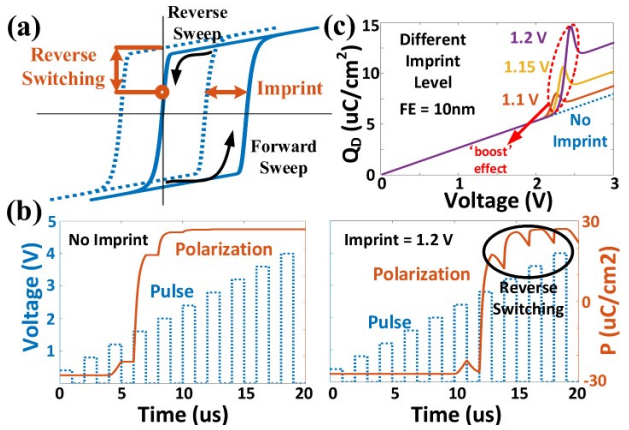

Fig. 3. Pulse measurement simulation results of a stand-alone FE capacitor. (a) Illustration of imprint and reverse switching. (b) Polarization as a function of time and pulse without (left frame) and with (right frame) imprint. (c) Q_D-V curves with different imprint levels.

Fig. 3(a) depicts the typical imprint behavior of a FE capacitor and its related reverse switching. The remnant polarization (polarization at V = 0) of the imprinted FE is smaller than that of the non-imprinted FE. When applied voltage drops to zero, there is a reverse polarization switching, as shown in Fig. 3(a). Fig. 3(b) shows the applied pulse and polarization as functions of time without (left frame) and with (right frame) imprint. The imprint-induced shift is set to be 1.2 V. As one can see, the ferroelectric with imprint clearly exhibits reverse switching at the falling edge of the pulse.

Fig. 3(c) shows the $Q_D - V$ curves of the ferroelectric with various imprint levels. Without imprint, no capacitance 'boost' effect is observed. With imprint, Q_D is 'boosted' when the pulse amplitude is high enough to trigger reverse switching, and the 'boost' effect is correlated with the imprint level. This 'boost' effect in a stand-alone imprinted BTO capacitor is shown in Fig.3(a) of [8], where the experimental $Q_D - V$ curve has the same trajectory as what we obtained in the simulation. Obviously, a stand-alone FE capacitor should not possess 'NC' effect according to the QSNC theory [1], and therefore the results point to imprint and reverse switching as the cause.

B. FE-DE Bilayer Capacitor

Fig. 4 shows the simulation results of a FE-DE bilayer capacitor with 10nm of HZO-based FE layer (without imprint). Fig. 4(a) shows the hysteresis loops of FE-DE bilayer capacitors with four different DE thicknesses. Due to the existence of the DE layer, the remnant polarization is lower than the saturated value, which enables reverse switching. For FE-DE capacitors, imprint is not necessary for reverse switching.

Fig. 4(b) shows the $Q_D - V$ curve of a FE-DE capacitor with 4nm DE. The dashed line represents the $Q - V$ of the DE capacitor alone. As one can see, the slope of the FE-DE surpasses that of the DE alone at high voltages, and the hysteresis is negligibly small. This is qualitatively similar to the results reported by Hoffman et. al. as depicted in their Fig. 12 in [9] and Fig. 3(g) in [10].

Fig. 4(c) above shows the polarization as a function of time and applied pulse. Initially, the remnant polarization is negative. With increasing pulse amplitude, polarization starts switching to positive. Before reaching positive remnant polarization, there is no reverse switching. After that,

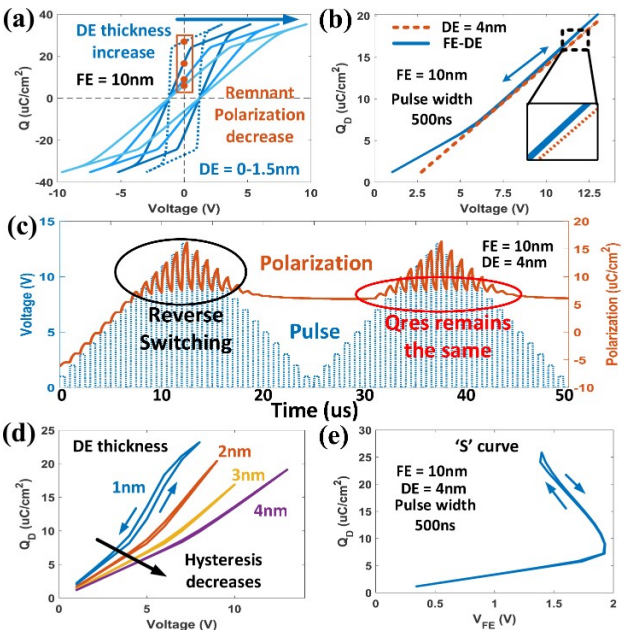

Fig. 4. Simulation results of FE-DE capacitor with 10nm of FE layer. (a) Hysteresis loops of FE-DE capacitors with 4 different DE thicknesses. (b) Simulated Q_D-V curves of an FE/DE and a DE capacitor. (c) Pulse string (blue) and polarization of the FE-DE capacitor (orange) as functions of time. (d) Simulated Q_D-V curves with four different DE thicknesses. (e) Q_D-'V_{FE}' curve extracted from Fig. 3 (b).

one starts to see reverse switching as well as the 'boost' effect. We applied the same pulse sequence for the second time, and Q_{res} remains the same. This result is consistent with Fig. 3(g) in [10]. Fig. 4(d) shows the $Q_D - V$ curves with four different DE thicknesses. For FE-DE capacitors with thinner DE layers, most of the voltages drop across the FE layers so that their polarizations reach saturation with smaller applied voltages. When polarization is saturated, the reverse switching is also saturated. Thus, the 'boost' effect disappears with higher voltages. Also, saturated polarization results in smaller hysteresis. This also explains why hysteresis decreases with thicker DE since the FE voltage is not large enough.

Fig. 4(e) shows the $Q_D -' V'_{FE}$ curve extracted from the $Q_D - V$ curve with 4nm of DE, where $'V'_{FE}$ is calculated by the equation $'V'_{FE} = V - Q_D/C_{DE}$. This $Q_D -' V'_{FE}$ curve 'matches' the extracted 'S' curve in [9], [10]. However, since the Landau switching model is not used at all in our simulation, the extracted 'S' curve we have obtained is not related to the 'S' curve arising from the Landau theory.

VI. Summary

We studied, by numerical simulation, the alleged capacitance 'boost' effect in FE-DE bilayer capacitors obtained by the pulse measurements. By the use of the Nucleation-Limited Switching (NLS) model for ferroelectric domain switching, and incorporating the commonly occurring imprint phenomenon for ferroelectric films, we have demonstrated that reverse switching at the falling edge during the pulse measurement is most likely responsible for the experimentally observed apparent 'NC' effects, without invoking the QSNC theory. This work provides a sensible alternative explanation of the experimentally observed capacitance 'boost' effects of imprinted FE capacitors and FE-DE bilayer capacitors obtained by use of the pulse measurements.

REFERENCES

[1] S. Salahuddin and S. Datta, "Use of negative capacitance to provide voltage amplification for low power nanoscale devices," *Nano Lett.*, vol. 8, no. 2, pp. 405–410, Feb. 2008, doi: 10.1021/nl071804g.

[2] A. I. Khan, K. Chatterjee, B. Wang, S. Drapcho, L. You, C. Serrao, S. R. Bakaul, R. Ramesh, and S. Salahuddin, "Negative capacitance in a ferroelectric capacitor," *Nature Mater.*, vol. 14, no. 2, pp. 182–186, Dec. 2014, doi: 10.1038/nmat4148.

[3] A. Islam Khan, D. Bhowmik, P. Yu, S. Joo Kim, X. Pan, R. Ramesh, and S. Salahuddin, "Experimental evidence of ferroelectric negative capacitance in nanoscale heterostructures," *Appl. Phys. Lett.*, vol. 99, no. 11, Sep. 2011, Art. no. 113501, doi: 10.1063/1.3634072.

[4] D. J. R. Appleby, N. K. Ponon, K. S. K. Kwa, B. Zou, P. K. Petrov, T. Wang, N. M. Alford, and A. O'Neill, "Experimental observation of negative capacitance in ferroelectrics at room temperature," *Nano Lett.*, vol. 14, no. 7, pp. 3864–3868, Jun. 2014, doi: 10.1021/nl5017255.

[5] K.-S. Li, P.-G. Chen, T.-Y. Lai, C.-H. Lin, C.-C. Cheng, C.-C. Chen, Y.-J. Wei, Y.-F. Hou, M.-H. Liao, M.-H. Lee, M.-C. Chen, J.-M. Sheih, W.-K. Yeh, F.-L. Yang, S. Salahuddin, and C. Hu, "Sub-60 mV-swing negative-capacitance FinFET without hysteresis," in *IEDM Tech. Dig.*, Dec. 2015, pp. 22.6.1–22.6.4, doi: 10.1109/IEDM.2015.7409760.

[6] A. I. Khan, K. Chatterjee, J. P. Duarte, Z. Lu, A. Sachid, S. Khandelwal, R. Ramesh, C. Hu, and S. Salahuddin, "Negative capacitance in short-channel FinFETs externally connected to an epitaxial ferroelectric capacitor," *IEEE Electron Device Lett.*, vol. 37, no. 1, pp. 111–114, Jan. 2016, doi: 10.1109/LED.2015.2501319.

[7] A. K. Yadav, K. X. Nguyen, Z. Hong, C. Hu, S. Das, P. García-Fernández, P. Aguado-Puente, C. T. Nelson, B. Prasad, D. Kwon, S. Cheema, A. I. Khan, J. Ìñiguez, J. Junquera, L.-Q. Chen, D. A. Müller, R. Ramesh, and S. Salahuddin, "Spatially resolved steady-state negative capacitance," *Nature*, vol. 565, no. 7740, pp. 468–471, Jan. 2019, doi: 10.1038/s41586-018-0855-y.

[8] Y. J. Kim, H. Yamada, T. Moon, Y. J. Kwon, C. H. An, H. J. Kim, K. D. Kim, Y. H. Lee, S. D. Hyun, M. H. Park, and C. S. Hwang, "Time-dependent negative capacitance effects in Al_2O_3/$BaTiO_3$ bilayers," *Nano Lett.*, vol. 16, no. 7, pp. 4375–4381, Jul. 2016, doi: 10.1021/acs.nanolett.6b01480.

[9] M. Hoffmann, B. Max, T. Mittmann, U. Schroeder, S. Slesazeck, and T. Mikolajick, "Demonstration of high-speed hysteresis-free negative capacitance in ferroelectric $Hf_{0.5}Zr_{0.5}O_2$," in *IEDM Tech. Dig.*, Dec. 2018, pp. 31.6.1–31.6.4, doi: 10.1109/IEDM.2018.8614677.

[10] M. Hoffmann, F. P. G. Fengler, M. Herzig, T. Mittmann, B. Max, U. Schroeder, R. Negrea, P. Lucian, S. Slesazeck, and T. Mikolajick, "Unveiling the double-well energy landscape in a ferroelectric layer," *Nature*, vol. 565, no. 7740, pp. 464–467, Jan. 2019, doi: 10.1038/s41586-018-0854-z.

[11] T. P. Ma and J.-P. Han, "Why is nonvolatile ferroelectric memory field-effect transistor still elusive?" *IEEE Electron Device Lett.*, vol. 23, no. 7, pp. 386–388, Jul. 2002, doi: 10.1109/LED.2002.1015207.

[12] N. Gong and T.-P. Ma, "Why is FE–HfO_2 more suitable than PZT or SBT for scaled nonvolatile 1-T memory cell? A retention perspective," *IEEE Electron Device Lett.*, vol. 37, no. 9, pp. 1123–1126, Sep. 2016, doi: 10.1109/LED.2016.2593627.

[13] C. Alessandri, P. Pandey, A. Abusleme, and A. Seabaugh, "Switching dynamics of ferroelectric Zr-doped HfO_2," *IEEE Electron Device Lett.*, vol. 39, no. 11, pp. 1780–1783, Nov. 2018, doi: 10.1109/LED.2018.2872124.

[14] J. Müller, T. S. Boscke, S. Müller, E. Yurchuk, P. Polakowski, J. Paul, D. Martin, T. Schenk, K. Khullar, A. Kersch, W. Weinreich, S. Riedel, K. Seidel, A. Kumar, T. M. Arruda, S. V. Kalinin, T. Schlosser, R. Boschke, R. van Bentum, U. Schroder, and T. Mikolajick, "Ferroelectric hafnium oxide: A CMOS-compatible and highly scalable approach to future ferroelectric memories," in *IEDM Tech. Dig.*, Dec. 2013, pp. 10.8.1–10.8.4, doi: 10.1109/IEDM.2013.6724605.

[15] F. P. G. Fengler, M. Hoffmann, S. Slesazeck, T. Mikolajick, and U. Schroeder, "On the relationship between field cycling and imprint in ferroelectric $Hf_{0.5}Zr_{0.5}O_2$," *J. Appl. Phys.*, vol. 123, no. 20, May 2018, Art. no. 204101, doi: 10.1063/1.5026424.

[16] Y. J. Kim, M. H. Park, W. Jeon, H. J. Kim, T. Moon, Y. H. Lee, K. D. Kim, S. D. Hyun, and C. S. Hwang, "Interfacial charge-induced polarization switching in Al_2O_3/Pb(zr,Ti)O_3 bi-layer," *J. Appl. Phys.*, vol. 118, no. 22, Dec. 2015, Art. no. 224105, doi: 10.1063/1.4937544.

[17] Y. J. Kim, M. H. Park, Y. H. Lee, H. J. Kim, W. Jeon, T. Moon, K. Do Kim, D. S. Jeong, H. Yamada, and C. S. Hwang, "Frustration of negative capacitance in Al_2O_3/$BaTiO_3$ bilayer structure," *Sci. Rep.*, vol. 6, no. 1, pp. 1–11, Jan. 2016, doi: 10.1038/srep19039.

[18] Z. D. Zhou and D. Y. Wu, "Domain structures of ferroelectric films under different electrical boundary conditions," *AIP Adv.*, vol. 5, no. 10, Oct. 2015, Art. no. 107206, doi: 10.1063/1.4933053.

[19] J. Wang, M. Kamlah, T.-Y. Zhang, Y. Li, and L.-Q. Chen, "Size-dependent polarization distribution in ferroelectric nanostructures: Phase field simulations," *Appl. Phys. Lett.*, vol. 92, no. 16, Apr. 2008, Art. no. 162905, doi: 10.1063/1.2917715.

[20] Y. L. Li, S. Y. Hu, Z. K. Liu, and L. Q. Chen, "Effect of electrical boundary conditions on ferroelectric domain structures in thin films," *Appl. Phys. Lett.*, vol. 81, no. 3, pp. 427–429, Jul. 2002, doi: 10.1063/1.1492025.